

# Periodic Operation of Trickle Bed Reactors: An Approach To Catalyst Design through Modeling at the Particle Scale

María A. Ayude,<sup>†</sup> Miryan C. Cassanello,<sup>‡</sup> Patricia M. Haure,<sup>†</sup> and Osvaldo M. Martínez<sup>\*,§</sup>

INTEMA, CONICET, UNMdP. J.B. Justo 4302, 7600 Mar del Plata, Argentina, PINMATE, Dep. Industrias, FCEyN-UBA Int. Güiraldes 2620, C1428BGA Buenos Aires, Argentina, and Dep. Ing. Química, FI-UNLP-CINDECA, Calle 47 No. 257, 1900 La Plata, Argentina

The behavior of an isothermal catalytic particle in a TBR with ON–OFF liquid flow modulation has been modeled considering isothermal conditions. The impact of catalytic properties has been investigated considering uniform and egg shell distributions. Furthermore, the effect of varying inert core porosity for egg shell catalysts has also been addressed. The model represents experimental trends observed for slow and intermediate cycling. In most cases, egg shell catalysts presented a better performance in comparison with uniform catalysts. However, during cycling, performance depends on working conditions and catalytic properties. Therefore, catalyst design and mode of operation are related issues that need to be defined jointly. The relevance of internal processes (reaction, diffusion, and accumulation) and external transport on overall performance has been addressed. Therefore, the model would serve as a basis, coupled with the development at reactor scale, for the integral reactor design.

## Introduction

Periodic operation of trickle bed reactors (TBRs) is an alternative to improve reactor performances. Even though TBRs are usually operated under steady-state conditions, many recent studies have shown experimentally that considerable reaction rate enhancement can be achieved through liquid flow modulation, switching periodically the loading between two predetermined levels while the gas flows continuously.<sup>1–3</sup>

Another alternative to enhance the performance of catalytic systems, including TBRs, is the design of tailored catalyst. Different catalytic particle size, geometric configuration, and active phase distribution may lead to more efficient catalysts. The impact of nonuniform activity catalysts on reactor performance had been extensively studied.<sup>4</sup> Several works reported the use of nonuniform active catalysts in TBRs under steady state<sup>5,6</sup> and with liquid flow modulation.<sup>7–9</sup> The most frequent arrangement is the so-called “egg-shell”, in which a thin layer of catalytic material is placed in the external surface of a spherical particle.

The use of models to evaluate the impact of both alternatives on TBRs performance could reduce significantly the experimental work. Gavriilidis et al.<sup>4</sup> presented a well recognized model to represent the steady-state behavior of nonuniform active catalyst. Also, several authors have modeled the steady-state behavior of TBRs loaded with egg shell catalyst.<sup>10–11</sup>

In the case of cycling, the factors governing the reaction rate present different dynamical responses to the liquid flow perturbation and interactions become quite complex. Thus, modeling is still a challenge. The behavior of an isothermal particle placed inside a TBR

in which liquid flow modulation is imposed is affected at two different levels: from mass transport and hydrodynamic processes that occur outside the particle and from mass transport, chemical reaction, and accumulation that take place inside the particle. The interaction of these effects in an integral TBR during cycling is complicated; thus, several authors had presented models considering only some of the events that affect reactor performance. Hydrodynamic processes require to be studied at the reactor level, taking into account the bed as a whole, even using a nonreacting system. On the other hand, for simplicity, processes occurring in the interior of the particle can be studied within a single particle.

Lange et al.<sup>12,13</sup> modeled the reactor taking into account hydrodynamic processes but neglecting internal mass transport resistances. With this simplification, changes in reaction rate and accumulation inside the particle cannot be evaluated. Stegasov et al.<sup>14</sup> developed a model that accounts extensively for hydrodynamic considerations but simplified the internal phenomena treatment through the definition of a steady-state effectiveness factor. This approach is difficult to justify because diffusion is important, and transients in the particles will be large in the flow interruption mode of operation. Therefore, these models are able to partially simulate the influence of liquid flow modulation on reactor performance, since they disregard the transient phenomena occurring inside the particle.

Alternatively, other studies have focused their attention on the internal phenomena, taking into account a single particle and considering specific external wetting and mass transport conditions. Boelhouwer<sup>15</sup> represented the catalyst as a vertical slab containing pores of  $10^{-4}$  m length. The catalytically active material was situated only inside the pores. The model accounts for mass transport and accumulation inside the pores but for a particular situation since the egg shell catalyst has an impermeable core. The model has been applied mainly to simulate an operation that alternates between

\* To whom correspondence should be addressed. Tel.: (+54-11)45763383. E-mail: phaure@fi.mdp.edu.ar/ommartin@volta.ing.unlp.edu.ar.

<sup>†</sup> INTEMA.

<sup>‡</sup> PINMATE.

<sup>§</sup> FI-UNLP-CINDECA.

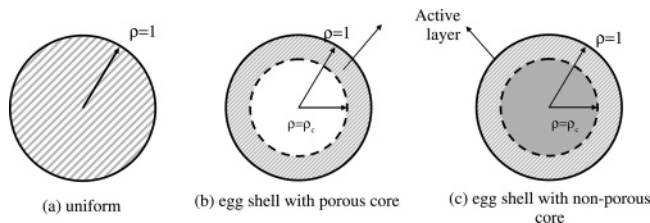


**Figure 1.** Schematic indication of catalyst particle configurations.

a low and a high liquid flow rate, generally termed BASE-PEAK operation.

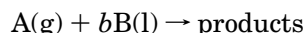
Kouris et al.<sup>16</sup> modeled the behavior of a single, uniform particle with partial external wetting, total internal wetting, and transport, reaction, and accumulation processes taking place inside the particle. Dynamic behavior of the particle was well represented by the model. However, since the objective of their study was to simulate the performance of catalytic particles in a TBR operating in the pulse-flow regime, external conditions differ from those in the periodic operation of TBRs. Thus, regardless of several efforts presented in the literature, a comprehensive, consistent model to represent the behavior of a particle in a TBR during cycling is not available.

Accordingly, the objective of the present contribution is to analyze the response of a single particle to temporal modifications of the external conditions. Results at the single particle cannot be compared with experimental outcomes of an integral reactor. However, this approach is still valuable since it allows decoupling essential components of the system to observe its response to temporal variations of several parameters. Uniform and egg shell particles, with different widths of active layer and permeable or impermeable core, will be considered in the analysis.

Results will contribute to analyze rigorously the impact of liquid flow modulation on internal particle behavior. Then, the model, coupled with the development at reactor scale,<sup>13</sup> would serve as a basis for the integral reactor design. In addition, it will provide a mean to judge if the performances of uniform and egg shell catalysts during steady state are still valid when liquid flow modulation is imposed.

## Model Development

A single reaction between a gaseous reactant (A) and a nonvolatile liquid reactant (B) within a porous solid catalyst is considered



Different catalyst particle configurations, with the same amount of active phase distributed in different reaction volumes, are examined (Figure 1).

The kinetic is assumed to be first-order with respect to each reactant, i.e., (1,1).

Isothermal conditions are assumed, to focus the analysis on the mass transport and accumulation effects. Non-steady-state mass balances for the gas and liquid reactants are formulated and solved for a spherical particle. External behavior during ON-OFF operation is described as a square-wave cycling.<sup>17</sup>

The model assumes that the external surface of the particle is completely wet during the ON cycle (also in the steady state taken as a reference) and completely dry during the OFF cycle. Even if these assumptions

limit the analysis to certain conditions, they strongly simplify the resolution time, and many of the qualitative conclusions can be extended to external partial wetting during the ON and OFF cycles. Once the liquid flow stops, the external mass transport resistances are considered negligible. This last assumption is supported by the significantly higher values of mass transfer coefficients in the gas phase, which would mostly determine the external resistances during the dry period of the cycle. This approach is valid if the time required to drain the particle is smaller than the extent of the dry cycle.

Taking into account these assumptions, the dimensionless differential mass balances for both reactants inside the catalyst are

$$\frac{\partial \alpha_A}{\partial \tau} = \frac{\partial^2 \alpha_A}{\partial \rho^2} + \frac{2}{\rho} \frac{\partial \alpha_A}{\partial \rho} - \phi^2 \cdot \alpha_A \cdot \alpha_B \quad (1a)$$

$$\frac{\partial \alpha_B}{\partial \tau} = \delta \cdot \left( \frac{\partial^2 \alpha_B}{\partial \rho^2} + \frac{2}{\rho} \frac{\partial \alpha_B}{\partial \rho} \right) - \phi^2 \cdot \xi \cdot \alpha_A \cdot \alpha_B \quad (1b)$$

Dimensionless parameters are

$$\rho = \frac{r}{R} \quad \alpha_A = \frac{C_A}{C_A^*} \quad \alpha_B = \frac{C_B}{C_{B0}} \quad \tau = \frac{t \cdot D_A}{\epsilon_p \cdot R^2} \quad \delta = \frac{D_B}{D_A} \\ \xi = \frac{b \cdot C_A^*}{C_{B0}}$$

To compare the performance of a catalyst with an active phase uniformly distributed over the whole particle, with results obtained with an egg shell distribution, the following condition is imposed to the kinetic constant

$$k_{es} = k_{un} \frac{V_{un}}{V_{es}} = k_{un} \cdot \frac{1}{(1 - \rho_c^3)} \quad \text{for } \rho_c \leq \rho \leq 1 \quad (2a)$$

$$k_{es} = 0 \quad \text{for } \rho < \rho_c \quad (2b)$$

where  $k_{un}$  and  $k_{es}$  are the kinetic constants for the uniform and egg shell distributions, respectively, and  $\rho_c$  is the dimensionless radius of the internal core of the particle without active phase (see Figure 1). Accordingly, the Thiele modulus is defined as

$$\phi^2 = \frac{k_{un} \cdot R^2 \cdot C_{B0}}{(1 - \rho_c^3) D_A} = \frac{\phi_{un}^2}{(1 - \rho_c^3)}$$

The catalyst with uniform activity is the specific case of  $\rho_c = 0$ . Therefore, two differential equations for the catalyst with uniform activity, four differential equations for the egg shell catalyst with porous core, and two differential equations for the egg-shell catalyst with nonporous core are defined.

Initial conditions for the whole catalyst particle are

$$\tau = 0 \quad \alpha_i = 1 \quad i = A, B \quad (3a)$$

Boundary conditions in the particles for the wet period of the cycling are

$$\rho = 1 \quad \frac{\partial}{\partial \rho} \alpha_A = \text{Bi}_{\text{gl},A} \cdot (1 - \alpha_A) \quad \frac{\partial}{\partial \rho} \alpha_B = \text{Bi}_{\text{ls},B} \cdot (1 - \alpha_B) \quad (3b)$$

where

$$Bi_{gl,A} = \frac{\left(\frac{1}{k_{lA} \cdot a_{gl}} + \frac{1}{k_{sA} \cdot a_p}\right)^{-1} \cdot R^2}{3 \cdot D_A} \quad Bi_{ls,B} = \frac{k_{sB} \cdot a_p \cdot R^2}{3 \cdot D_B}$$

Equations 3a and 3b are valid for all the catalysts. The other boundary conditions depend on the type of catalyst.

Catalyst with uniform activity:

$$\rho = 0 \quad \frac{\partial}{\partial \rho} \alpha_i = 0 \quad i = A, B \quad (3c)$$

Egg shell catalyst with porous core:

$$\rho = 0 \quad \frac{\partial}{\partial \rho} \alpha_i = 0 \quad i = A, B \quad (3d)$$

$$\rho = \rho_c \quad \alpha_i|_{\rho_c^-} = \alpha_i|_{\rho_c^+} \quad i = A, B \quad (3e)$$

$$\rho = \rho_c \quad \frac{\partial \alpha_i}{\partial \rho}|_{\rho_c^-} = \frac{\partial \alpha_i}{\partial \rho}|_{\rho_c^+} \quad i = A, B \quad (3f)$$

Egg shell catalyst with nonporous core:

$$\rho = \rho_c \quad \frac{\partial}{\partial \rho} \alpha_i = 0 \quad i = A, B \quad (3g)$$

For the period in which the liquid is cut off, the boundary conditions are the same, except for eq 3b, which becomes

$$\rho = 1 \quad \alpha_A = 1 \quad \frac{\partial}{\partial \rho} \alpha_B = 0 \quad (3h)$$

The boundary conditions required for solving the model under steady-state operation are (3b)–(3g), according to the catalyst employed.

The model is solved by explicit finite differences. Several discretization strategies were tested to verify convergence of the results. From reactants radial profiles within the catalyst, instantaneous overall efficiencies during the wet ( $\eta_{ON}$ ) and dry ( $\eta_{OFF}$ ) cycles can be calculated as

$$\eta_i = \frac{3 \int_{\rho_c}^1 \rho^2 \cdot \alpha_A \cdot \alpha_B \cdot d\rho}{(1 - \rho_c^3)} \quad i = ON, OFF, ss \quad (4)$$

where the reference reaction rate, used to calculate overall effectiveness factors, is evaluated taking into account the bulk phase concentrations.

The overall effectiveness factor for the cycle invariant state,  $\eta_{cyc}$ , may be defined as

$$\eta_{cyc} = \frac{\int_0^{\tau_{ON}} \eta_{ON} \cdot d\tau + \int_0^{\tau_{OFF}} \eta_{OFF} \cdot d\tau}{\tau_{ON} + \tau_{OFF}} \quad (5)$$

where  $\tau_{ON}$  and  $\tau_{OFF}$  are the times in which the liquid is ON and OFF.

An enhancement factor ( $\epsilon$ ) due to periodic operation can thus be defined. It is based on the steady-state overall effectiveness factor evaluated at the mean liquid velocity ( $\eta_{ss}$ ) as

$$\epsilon = \eta_{cyc} / \eta_{ss} \quad (6)$$

**Table 1. Characteristics of Catalyst Employed in the Simulation**

catalyst <sup>a</sup>	distribution of activity	active layer width <sup>b</sup>	nonactive core
UN	uniform	100	
ES10P	egg shell	10	porous
ES1P	egg shell	1	porous
ES10NP	egg shell	10	nonporous
ES1NP	egg shell	1	nonporous

<sup>a</sup>  $R = 0.001$  m;  $D_A = 5.35 \times 10^{-10}$  m<sup>2</sup>/s. <sup>b</sup> As a percentage of the particle radius.

To compare results, the relationship between the liquid velocity for steady-state operation ( $u_{LSS}$ ) and during the ON cycle of periodic operation ( $u_{LON}$ ) is taken into account as

$$u_{LON} = u_{LSS} \cdot (1/s) \quad (7)$$

where the split ( $s$ ) is the fraction of the cycle period during which there is liquid circulation across the bed.

Mass transfer coefficients for the ON cycle would depend on the split according to

$$k_{ION} = k_{iss} \cdot (1/s)^{\gamma_1} \quad (8a)$$

$$k_{sON} = k_{sss} \cdot (1/s)^{\gamma_2} \quad (8b)$$

This dependence will be reflected in the corresponding Biot values. The exponents,  $\gamma_1$  and  $\gamma_2$ , indicate the influence of the liquid velocity on each mass transfer coefficient and their value depend on the flow regime and on the correlation used to estimate them. Considering trickle flow around the particle, the correlation proposed by Goto and Smith<sup>18</sup> can be used, with  $\gamma_1 = 0.41$  and  $\gamma_2 = 0.56$ .

For comparison purposes, a zero-order kinetics with respect to B is assumed for some conditions, i.e (1,0). In this case,  $\alpha_B$  is substituted in eqs (1) and (4), by the Heaviside function,  $H(\alpha_B)$ :

$$H(\alpha_B) = \begin{cases} 0 & \text{if } \alpha_B \leq 0 \\ 1 & \text{if } \alpha_B > 0 \end{cases}$$

The definition of Thiele modulus becomes  $\phi^2 = k_{un} \cdot R^2 / (1 - \rho_c^3) D_A = \phi_{un}^2 / (1 - \rho_c^3)$ .

## Results and Discussion

Steady-state reference results presented here were evaluated at complete external wetting conditions ( $f=1$ ), considering  $Bi_{ls,B} = 50$  and  $Bi_{gl,A} = 5$ . The influence of these parameters on the behavior of a uniform catalyst particle has been recently evaluated.<sup>17</sup> Table 1 summarizes the different catalyst configurations studied in the present work.

Reactant concentration profiles inside the particle change with time and with the external conditions imposed. Invariant concentration profiles at the end of ON and OFF cycles are achieved after 10–30 cycles, depending on operating conditions.

Gas (A) and liquid (B) reactant profiles inside catalysts UN and ES10P are shown in Figure 2a–d, at the end of both the wet and dry cycles. Additionally, the evolution of gaseous reactant profiles during the dry cycle is also shown. For both catalysts during the wet cycle, the concentration of A at the catalyst surface is lower than the bulk concentration of A, due to the gas–

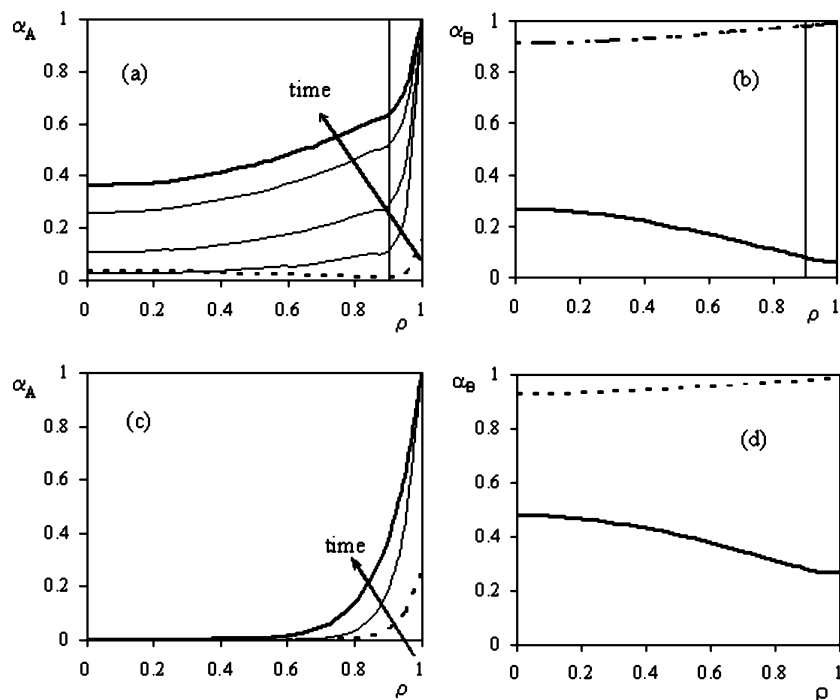


**Figure 2.** Reactant concentration profiles during cycling for ES10P (a and b) and UN catalyst (c and d) at the end of wet (---) and dry (—) cycles.  $P$ : 0.64;  $\phi_{un} = 20$ ;  $s = 0.5$ ;  $Bi_{gl,s,A} = 5$ ;  $Bi_{ls,B} = 50$ ;  $\xi = 1/20$ ;  $\delta = 1$ .

liquid mass transfer resistance. Since the liquid–solid resistance is small, the liquid reactant concentration at the catalyst surface is close to the liquid bulk concentration.

During the dry cycle, the surface concentration of A equals the saturation value since external mass transfer resistances become negligible for both catalysts. Reactant A is completely consumed for certain locations in the uniform catalyst, whereas in the egg shell catalyst, A is not depleted. For the egg shell, accumulation of A in the core of the catalyst is observed during the dry cycle: although the local catalyst activity is increased due to the higher number of active sites per unit volume, the active shell width is not thick enough to consume A in any point. During the wet cycle, the accumulated A diffuses toward the reaction zone, decreasing its internal concentration, but it may not be totally consumed. Larger density of active sites and accumulation of A contribute to the overall reaction rate enhancement during the wet cycle.

The liquid reactant B is not fed during the dry period, and it is also consumed more readily at the outer layer of the catalyst due to the higher concentration of A, hence its concentration decreases in that direction (Figure 2b,d). If the dry cycle is long enough, the concentration of B within the catalyst decreases considerably for certain locations. A region of the catalyst with a small concentration of B diminishes the overall effectiveness factor. Liquid reactant B is consumed more rapidly in the egg shell, due to the higher catalyst activity.

Accumulation processes are clearly visualized. Within both catalysts, the liquid reactant accumulates during the wet cycle. Conversely, the gas reactant accumulates during the dry cycle only for the egg shell catalyst. This fact had a remarkable importance on cycling performance and will be discussed later.

The enhancement factor due to periodic operation ( $\epsilon$ ) for both catalysts is shown in Figure 3a as a function of cycle splits for different periods. A maximum is always present in the enhancement vs split curve. This trend

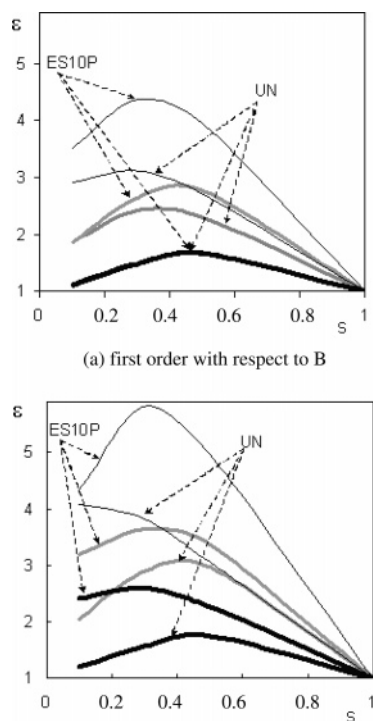


**Figure 3.** Enhancement factor due to periodic operation ( $\epsilon$ ) vs split for ES10P and UN catalyst for different cycle periods (—,  $P = 0.16$ ; grey line,  $P = 0.64$ ; thick black line,  $P = 1.6$ ).  $\phi_{un} = 20$ ;  $Bi_{gl,s,A} = 5$ ;  $Bi_{ls,B} = 50$ ;  $\xi = 0.05$ ;  $\delta = 1$ .

has been experimentally observed by several authors,<sup>9,19–20</sup> including those that used egg shell catalysts. As the split diminishes, the duration of the dry cycle increases, favoring the access of A. However, if the split is small, replenishment of B during the wet cycle will not be complete, and its concentration inside the particle will be lower. This will decrease the reaction rate, and the enhancement will also diminish. The maximum moves toward smaller values as the period is reduced. When the dry period is too long (at higher periods or



smaller splits), B concentration inside the particle becomes very small, and the reaction rate drops off. Under these conditions enhancement due to cycling may be negligible.

Comparison between both catalysts shows that the predicted enhancement for the egg-shell catalyst is generally higher, although this type of configuration has a larger overall effectiveness factor for the reference steady state. The last is calculated for a similar particle with complete external mass transfer coefficients evaluated at the liquid velocity given by eq 7. However, the difference between both catalysts depends on the period and the split.

Liquid flow modulation increases the mass transfer of A to the particle and leads to higher improvements for the egg-shell type catalysts. This may be attributed to the same reasons that induce differences between egg shell and uniform configurations at steady-state conditions.<sup>4</sup> However, this explanation reflects the results achieved with cycling only if B concentration does not decrease too much during the dry cycle within the reaction zone. This condition is fulfilled for short and intermediate cycle periods and relatively high splits.

For long cycle periods at any split (as indicated in the lower curve of Figure 3a) or for very small splits, cycling enhancements for nonuniform and uniform catalysts may be similar. The duration of the OFF cycle negatively affects egg shell and uniform performances, but the effect is more pronounced for nonuniform catalysts. In them, during the OFF cycle, reactant B slowly diffuses from the catalyst center to the reaction zone. The uniform configuration will have reaction inside the catalyst at relatively large rates, since A penetrates further during the OFF period to regions where B is accumulated. The interaction of these two effects explains the curves illustrated in Figure 3a and the shift in maximum values found for both types of catalysts.

Comparison of outcomes obtained with different kinetic expressions was also done. Figure 3b shows results for a reaction that is first order with respect to A and zero order with respect to B. The curves are similar to those previously described, although variations are steeper because the kinetic does not depend on the liquid reactant concentration, thus the reaction rate does not decrease as B concentration diminishes. The reaction rate stops only when the concentration of B equals zero, starting at the external border of the particle during the dry cycle. Concepts exposed to explain the results shown in Figure 3a are valid in understanding the curves in Figure 3b. Comparison between both catalysts shows that, for the conditions examined, the egg shell catalyst presents a higher enhancement and the difference with the uniform catalyst is greater for the reaction that is zero order in B. This is explained taking into account the events occurring during the dry cycle when the concentration of B at the external border is relatively small. Therefore, the reaction rate will decrease when the order depends on B but will remain constant until  $\alpha_B$  is zero, for a reaction that is zero order with respect to B.

From the discussion presented above, it becomes clear that internal processes dynamic strongly affects the behavior of a catalytic particle. Hence, it has to be taken into account for modeling liquid flow modulation.

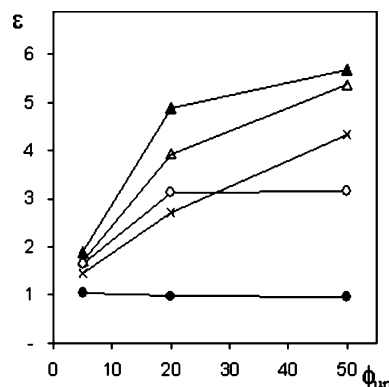


**Figure 4.** Enhancement factor due to periodic operation ( $\epsilon$ ) for a different catalyst distribution and a different Thiele modulus.  $\times$  UN;  $\triangle$  ES10P;  $\blacktriangle$  ES1P;  $\circ$  ES10NP;  $\bullet$  ES1NP.  $P$ : 0.16;  $s$  = 0.5;  $Bi_{gl,A}$  = 5;  $Bi_{ls,B}$  = 50;  $\xi$  = 1/20;  $\delta$  = 1.

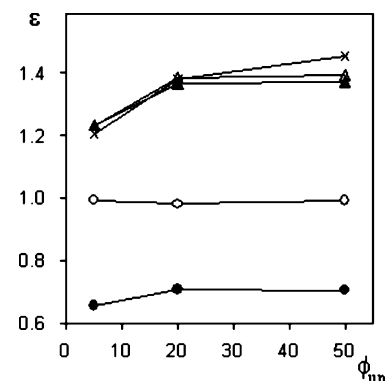


**Figure 5.** Enhancement factor due to periodic operation ( $\epsilon$ ) for a different catalyst distribution and a different Thiele modulus.  $\times$  UN;  $\triangle$  ES10P;  $\blacktriangle$  ES1P;  $\circ$  ES10NP;  $\bullet$  ES1NP.  $P$ : 0.16;  $s$  = 0.5;  $Bi_{gl,A}$  = 5;  $Bi_{ls,B}$  = 50;  $\xi$  = 1/2;  $\delta$  = 1.

Figures 4 and 5 show the enhancement factor evaluated for a different Thiele modulus. Also, the catalyst design is considered by taking into account particles with characteristics presented in Table 1.

Figure 4 shows that the enhancement of completely porous catalysts (UN, ES10P and ES1P) increases for a higher Thiele modulus,  $\phi$ . Under the conditions studied, this trend is observed regardless of the catalytic site distribution. At smaller values of the Thiele modulus, the enhancement will be lower in any case. The maximum on the enhancement vs split curve depends on the Thiele modulus,<sup>17</sup> and its location moves toward higher splits for larger values of  $\phi$ . Therefore, it can be verified that, for certain combinations of period and split, the tendency observed with a Thiele modulus can reverse. For the conditions studied, egg shell catalysts present higher enhancements than uniform catalysts. Comparison between egg shell catalysts indicates that the better enhancement is obtained for catalyst ES1P, which has the thinner active layer.

Results obtained with egg shell catalysts with a nonporous core (ES10NP and ES1NP) are also shown in Figure 4. These catalysts were used in models for a steady-state system<sup>11</sup> and for liquid flow modulation.<sup>15</sup>

Performances of egg shell catalysts with a porous and nonporous core show a remarkable difference, especially for the catalyst that holds the thinner active layer. When the core is porous, it acts as a reservoir of the liquid reactant, and this fact is responsible for the different results observed so far. Between nonporous

catalysts, differences arise from the higher storage capacity of the active layer of the ES10NP.

These results emphasize the influence of the inert core porosity of a catalyst, which should be taken into account for catalyst design and modeling of periodic operation. Even if egg shell type catalysts with porous and nonporous cores will render similar results for steady-state operation, the performance will be completely different for periodic operation. Therefore, the porous condition of the inert core should be clearly identified.

Another important factor to consider is the type of liquid flow modulation imposed. For ON–OFF operation (as analyzed here), B comes exclusively from accumulation in the pores during the OFF portion of the cycle. In BASE-PEAK operation, the access of B from the exterior is reduced during the BASE portion of the cycle but never runs down.<sup>15</sup> Therefore, positive enhancement is likely, even for an egg shell with nonporous core catalysts.

An additional significant conclusion of the results shown in Figure 4 is related to the modeling of periodic operation in TBRs. A frequent assumption is to ignore the accumulation inside the inert core for egg shell type catalysts. However, if the storage is ignored, the egg shell catalyst will resemble a nonporous core one. The accumulation inside the particle has a remarkable incidence and cannot be ignored when the catalyst is completely porous.

Finally, Figure 5 presents enhancements obtained with a ratio of reactants initial concentrations  $\xi = b \cdot C_{A^*}/C_{B_0} = 0.5$ , while other conditions remain constant. This situation can be achieved, for instance, by working at a different pressure. Completely porous catalysts (uniform and egg shell) have similar enhancement values. Only for the higher Thiele modulus investigated, catalyst UN presents a slightly higher performance. As exposed previously, this can be explained by taking into account the storage of B during the ON cycle and its subsequent diffusion and reaction during the OFF period. More significant differences are observed with nonporous core catalysts. Enhancement values are smaller than one, particularly for the ES1NP catalyst. In this case, the effectiveness factor at ON–OFF operation is even smaller than the effectiveness factor obtained for UN at steady-state operation. Naturally, cycling is not recommended under these conditions.

Comparison between uniform and egg shell catalysts for steady-state two-phase systems has been extensively studied.<sup>21</sup> The analysis can be easily extended to three phase systems. For a first-order kinetics, Morbidelli and Varma<sup>21</sup> have presented analytical expressions to evaluate the performance of egg shell catalysts. Their results indicate that the egg shell catalysts will always have a better performance, in comparison with uniform catalysts. However, the ratio of both effectiveness factors obtained depends on the values of the Thiele modulus and Biot numbers. For example, when internal and external resistances are large (i.e., Thiele = 50 and Biot = 5) and the egg shell catalyst has a thin active layer (active layer = 0.1 dimensionless), nonuniform and uniform effectiveness factors differ slightly (4.8%). So, under these conditions, both catalysts will perform alike. On the other hand, if external resistances are negligible (large Biot numbers), and for Thiele = 50, the difference between the effectiveness factor is quite important

**Table 2. Ratio of Effectiveness Factor between Catalyst with Egg Shell and Uniform Activity for Steady-State or Periodic Operation<sup>a</sup>**

case	$\phi_{un} = 5$	$\phi_{un} = 20$	$\phi_{un} = 50$
$\eta_{ES10P}/\eta_{UN}$ (SS)	1.2747	1.0760	1.0533
$\eta_{ES10P}/\eta_{UN}$ (P=0.16)	1.5044	1.5677	1.2952
$\eta_{ES1P}/\eta_{UN}$ (SS)	1.3792	1.1751	1.0761
$\eta_{ES1P}/\eta_{UN}$ (P=0.16)	1.7988	2.1195	1.4079

<sup>a</sup> Conditions: split: 0.5;  $Bi_{is,B} = 50$ ;  $Bi_{gl,A} = 5$ ,  $\xi = 0.05$ .

(94%). So, egg shell catalysts are clearly preferred under such conditions.

Periodic operation improvements are generally related to the temporal reduction of the external mass transport resistances. This may lead to substantial differences between uniform and egg shell catalysts performances during steady-state or periodic operation.

Table 2 compares effectiveness factors for different catalysts during steady state and ON–OFF liquid flow modulation, for a (1,1) kinetic. For steady-state operation, egg shell catalysts will perform slightly better than uniform catalysts, especially at a higher Thiele modulus, i.e., 20 or 50. However, during liquid flow modulation, the situation changes and egg shell catalysts present an important improvement in comparison with uniform catalysts. These results remark the importance of a simultaneous design of catalysts and type of operation.

## Conclusions

The behavior of a catalytic particle in a TBR with an ON–OFF liquid flow modulation has been modeled considering isothermal conditions and a (1,1) or (1,0) reaction kinetics. The impact of catalytic properties had been investigated considering uniform and egg shell distributions. Furthermore, the effect of varying inert core permeability for egg shell catalysts had also been addressed.

The model is able to describe experimental trends observed for slow and intermediate cycling. The enhancement vs split curve presents a maximum at intermediate splits. Its location depends on system parameters. Analogous trends were obtained for the kinetics examined.

Egg shell catalysts presented a better cycling performance in comparison with uniform catalysts. However, as in steady-state operation, performance depends on working conditions, catalytic properties, and on the type of liquid flow modulation imposed. Therefore, catalyst design and mode of operation are related issues that need to be defined jointly.

Even for conditions that lead to a similar performance of egg shell and uniform catalyst under steady-state operation, considerable differences may arise when liquid flow modulation is imposed. This is more relevant when internal and external mass transport resistances are significant.

Comparison between performances of egg shell catalysts with porous and nonporous inert core brings about interesting conclusions. At steady state, the nature of the inert core has no incidence on performance. However, with liquid flow interruption, differences become significant. The liquid reactant accumulates in the permeable core during the ON cycle and then diffuses and reacts in the OFF cycle.

The relevance of internal processes (reaction, diffusion, and accumulation) and external transport on overall performance has been addressed. Internal limi-

tations can be overcome with an appropriate catalyst design. External resistances may be reduced with liquid flow modulation. To elucidate whether periodic operation will lead to significant performance enhancement, internal processes had to be considered. To decide cycling strategies, a proper description of reactor hydrodynamics is required. The appropriate representation of both processes will provide a useful tool to understand experimental studies and to set suitable conditions for reactor design and its operation.

### Acknowledgment

Financial support from CONICET, UBA, UNMdP, UNLP, ANPCyT, and Fundación Antorchas are gratefully acknowledged.

### Nomenclature

$a_{gl}$  = gas-liquid interfacial area per unit volume of catalyst particle ( $m^{-1}$ )

$a_p$  = external surface area per unit volume of catalyst particle ( $m^{-1}$ )

$b$  = stoichiometric coefficient

$C$  = concentration (M)

$D$  = effective diffusivity ( $m^2/s$ )

$k$  = reaction rate constant

$k_l$  = overall gas liquid mass transfer coefficient (m/s)

$k_s$  = liquid to particle mass transfer coefficient (m/s)

$P$  = dimensionless cycle period

$r$  = radial variable in the catalyst (m)

$R$  = radius of the catalyst particle (m)

$s$  = split

$t$  = time (s)

$u$  = velocity (m/s)

$V$  = dimensionless active layer volume

### Greek letters

$\alpha$  = dimensionless reactant concentration

$\delta$  = model parameter ( $=D_B/D_A$ )

$\epsilon_p$  = porosity in the catalyst particle

$\epsilon$  = enhancement factor (defined by eq 6)

$\phi$  = Thiele modulus

$\eta$  = overall effectiveness factor (defined by eqs 4 and 5)

$\rho$  = dimensionless radial variable in the catalyst

$\tau$  = dimensionless time ( $=t \cdot D_A / (R^2 \cdot \epsilon_p)$ )

$\xi$  = model parameter ( $=b \cdot C_A^* / C_{B0}$ )

### Subscripts

0 = initial value

A = gaseous reactant

B = nonvolatile reactant

c = dimensionless radius of the nonactive core

cyc = cycling

es = egg shell catalyst

L = liquid

OFF = nonwet cycle

ON = wet cycle

ss = steady state

un = uniform active catalyst

### Superscripts

\* = saturation value

### Literature Cited

(1) Khadilkar, M.; Al-Dahhan, M. H.; Dudukovic, M. P. Parametric study of unsteady-state flow modulation in trickle-bed reactors. *Chem. Eng. Sci.* **1999**, *54*, 2585–2595.

(2) Silveston, P. L.; Hanika, J. Challenges for the periodic operation of trickle-bed catalytic reactors. *Chem. Eng. Sci.* **2002**, *57*, 3373–3385.

(3) Muzen, A.; Fraguó, M. S.; Cassanello, M. C.; Ayude, M. A.; Haure, P.; Martínez, O. M. Clean Oxidation of Alcohols in a Trickle-Bed Reactor with Liquid Flow Modulation. *Ind. Eng. Chem. Res.* **2005**, in press.

(4) Gavriilidis, A.; Varma, A.; Morbidelli, M. Optimal distribution of catalyst in pellets. *Catal. Rev. - Sci. Eng.* **1993**, *35*, 399–456.

(5) Mills, P. L.; Dudukovic, M. P. A comparison of current models for isothermal trickle-bed reactors. Application to a model reaction system. Chemical and Catalytic Reactor Modeling. *ACS Symp. Ser.* **1984**, *237*, 37–59.

(6) An, W.; Zhang, Q.; Ma, Y.; Chuang, K. T. Pd-based catalysts for catalytic wet oxidation of combined Kraft pulp mill effluents in a trickle bed reactor. *Catal. Today* **2001**, *64*, 289–296.

(7) Gabarain, L.; Castellari, A.; Cechini, J.; Tobolski, A.; Haure, P. M. Analysis of rate enhancement in a periodically operated trickle-bed reactor. *AIChE J.* **1997**, *43*, 166–172.

(8) Houserová, P.; Hanika, J. Experiments with periodically operated liquid feed stream. Proc. of CHISA 2002-15th Int. Congress of Chemical and Process Eng., Prague, Czech Republic, 2002.

(9) Bancho, M.; Manna, L.; Sicardi, S.; Ferri, A. Experimental investigation of fast-mode liquid modulation in a trickle-bed reactor. *Chem. Eng. Sci.* **2004**, *59*, 4149–4154.

(10) Beaudry, E. G.; Duduković, M. P.; Mills, P. L. Trickle-bed reactors: liquid diffusional effects in a gas-limited reaction. *AIChE J.* **1987**, *33*, 1435–1447.

(11) Harold, M. P.; Ng, K. M. Effectiveness enhancement and reactant depletion in a partially wetted catalyst. *AIChE J.* **1987**, *33*, 1448–1465.

(12) Lange, R.; Gutsche, R.; Hanika, J. Forced periodic operation of a trickle-bed reactor. *Chem. Eng. Sci.* **1999**, *54*, 2569–2573.

(13) Lange, R.; Schubert, M.; Dietrich, W.; Grunewald, M. Unsteady-state operation of trickle-bed reactors. *Chem. Eng. Sci.* **2004**, *59*, 5355–5361.

(14) Stegasov, A. N.; Kirillov, V. A.; Silveston, P. L. Modeling of catalytic SO<sub>2</sub> oxidation for continuous and periodic liquid flow through a trickle bed. *Chem. Eng. Sci.* **1994**, *49*, 3699–3710.

(15) Boelhouwer, J. G. Nonsteady operation of trickle-bed reactors: Hydrodynamics, mass and heat transfer, Ph.D. Thesis, Technische Universiteit Eindhoven, The Netherlands, 2001.

(16) Kouris, Ch.; Neophytides, St.; Vayenas, C. G.; Tsamopoulos, J. Unsteady state operation of catalytic particles with constant and periodically changing degree of external wetting. *Chem. Eng. Sci.* **1998**, *53*, 3129–3142.

(17) Ayude, M. A.; Cassanello, M. C.; Martínez, O. M.; Haure, P. M. Phenomenological approach to interpret the effect of liquid flow modulation in trickle-bed reactors at the particle scale. *Chem. Eng. Sci.* **2005**, in press.

(18) Goto, S.; Smith, J. M. Trickle-bed reactor performance: 1. Hold-up and mass transfer effects. *AIChE J.* **1975**, *21*, 706–713.

(19) Lange, R.; Hanika, J.; Stradiotto, D.; Hudgins, R. R.; Silveston, P. L. Investigations of periodically operated trickle-bed reactors. *Chem. Eng. Sci.* **1994**, *49*, 5615–5622.

(20) Skala, D.; Hanika, J. Periodic operations of trickle-bed reactor. Proc. of CHISA 2002-15th Int. Congress of Chemical and Process Eng., Prague, Czech Republic, 2002.

(21) Morbidelli, M.; Varma, A. On shape normalization for nonuniformly active catalyst pellets-II. *Chem. Eng. Sci.* **1983**, *38*, 297.

Received for review February 28, 2005  
Revised manuscript received May 26, 2005  
Accepted June 22, 2005

IE0502741